



# Visualizing the genome in high resolution challenges our textbook understanding

Melike Lakadamyali<sup>1,2</sup>✉ and Maria Pia Cosma<sup>3,4,5,6,7</sup>

The relationship between the 4D folding of the genome and its function is an outstanding question in biology. A range of methods that probe the folding of the genome in space and time with unprecedented resolution have been developed. These methods, including chromosome conformation capture and high-resolution light and electron microscopy, are shedding new light on genome architecture and function. Here, we review the emerging picture of genome organization revealed by super-resolution and live-cell imaging. We compare and contrast population-based chromosome conformation capture approaches and imaging-based approaches and highlight future challenges.

Human DNA is 2 m long. How this DNA undergoes enormous compaction to fit into the tiny space of a cell's nucleus (~20 µm in diameter) has been among the major mysteries of cell biology. It has been known for decades that repeating units of nucleosomes (146 bp of DNA wrapped around a core octamer of histone proteins) organize into 10-nm "beads on a string". However, further compaction is needed to fit the DNA into the nucleus. The longstanding model posits that chromatin folds into higher-order structures in a hierarchical manner, which includes the folding of the 10-nm fibers into 30-nm fibers by the linker histone H1 and subsequent folding into larger structures<sup>2</sup>.

Histones, in addition to compacting DNA, can also actively control gene expression through post-translational modifications to their tails that collectively generate an epigenetic "histone code"<sup>3</sup>. Specific histone 'marks' correlate with active versus silenced regions of the genome and hence are thought to give rise to different levels of chromatin compaction and higher-order structure<sup>3</sup>. That being said, a portion of the genome seems to contain unmodified histones<sup>4,5</sup>, and repressive histone marks can sometimes also be found in active promoters<sup>6</sup>, underscoring the need for better tools to visualize and map the precise relationship between histone marks, genome structure and function.

With the advent of new imaging and genomic technologies, we are now at an exciting time in history, in which the *in vivo* organization of the genome is being visualized at an unprecedented level of detail, overwriting our existing textbook models.

## Genome organization using chromosome conformation capture

Elucidating the physical structure of chromosomes is challenging because the relevant length scales are small. Nucleosomes are only 10 nm and <200 bp in size, the highly compacted fibers postulated by the textbook model are not much larger, and individual genes can be as small as few kilobases, containing only tens of nucleosomes. Our microscopic understanding of chromosome organization in the interphase nucleus has been limited by the low spatial resolu-

tion of a light microscope (250–400 nm) compared to the size of a nucleosome (~10 nm). Hence, until recently, our light microscopic understanding of genome organization in intact nuclei was limited to the observation that individual chromosomes occupy specific regions within the nucleus, so-called chromosome territories (of micrometer length scale; Fig. 1)<sup>7</sup>. In addition, heterochromatic and gene-poor chromosomes are enriched at the nuclear periphery and around nucleoli<sup>8,9</sup>, whereas gene-rich chromosomes tend to be within the nuclear interior<sup>9</sup>. Upon activation, genomic regions decondense and loop out of chromosome territories<sup>10</sup>. These observations suggested that chromosomes are not randomly organized inside the nucleus and that nuclear organization is important for gene activity, yet deciphering 3D genome folding at length scales relevant for gene activity has been hindered by the lack of appropriate tools.

The development of chromosome conformation capture (3C)<sup>11</sup>, as well as methods such as chromatin immunoprecipitation sequencing (ChIP-seq)<sup>12</sup>, has therefore been revolutionary, allowing us to map DNA contacts, epigenetic modifications and chromatin-binding proteins genome wide and relate these to the 3D genome organization at high-base-pair resolution. The working principles of these genomic methods have been reviewed elsewhere<sup>11,12</sup>. The resolution of the 3C methods depends on several factors, including crosslinking efficiency, frequency of restriction cutting and sequencing depth, and can range from 1 kb to 1 Mb<sup>13,14</sup>. These methods have confirmed many of the observations from fluorescence microscopy, such as the existence of chromosome territories<sup>14,15</sup>. Additionally, the high-throughput Hi-C method combined with deep sequencing has revealed several levels of organizational units of the genome, including so-called A and B compartments corresponding to active euchromatin and silenced heterochromatin; topologically associating domains (TADs), megabase-sized regions of the genome characterized by more abundant intra-TAD compared to inter-TAD interactions (Fig. 1); and sub-TADs and loops, self-associating physical domains at smaller length scales<sup>16</sup>. These organizational units in part help bring promoters into close contact

<sup>1</sup>Department of Physiology, University of Pennsylvania, Perelman School of Medicine, Philadelphia, PA, USA. <sup>2</sup>Department of Cell and Developmental Biology, University of Pennsylvania, Perelman School of Medicine, Philadelphia, PA, USA. <sup>3</sup>Centre for Genomic Regulation (CRG), The Barcelona Institute of Science and Technology, Barcelona, Spain. <sup>4</sup>Universitat Pompeu Fabra (UPF), Barcelona, Spain. <sup>5</sup>ICREA, Barcelona, Spain. <sup>6</sup>Guangzhou Regenerative Medicine and Health Guangdong Laboratory (GRMH-GDL), Guangzhou, China. <sup>7</sup>Key Laboratory of Regenerative Biology and Guangdong Provincial Key Laboratory of Stem Cells and Regenerative Medicine, Guangzhou Institutes of Biomedicine and Health, Chinese Academy of Science, Guangzhou, China.  
✉e-mail: melikel@pennmedicine.upenn.edu

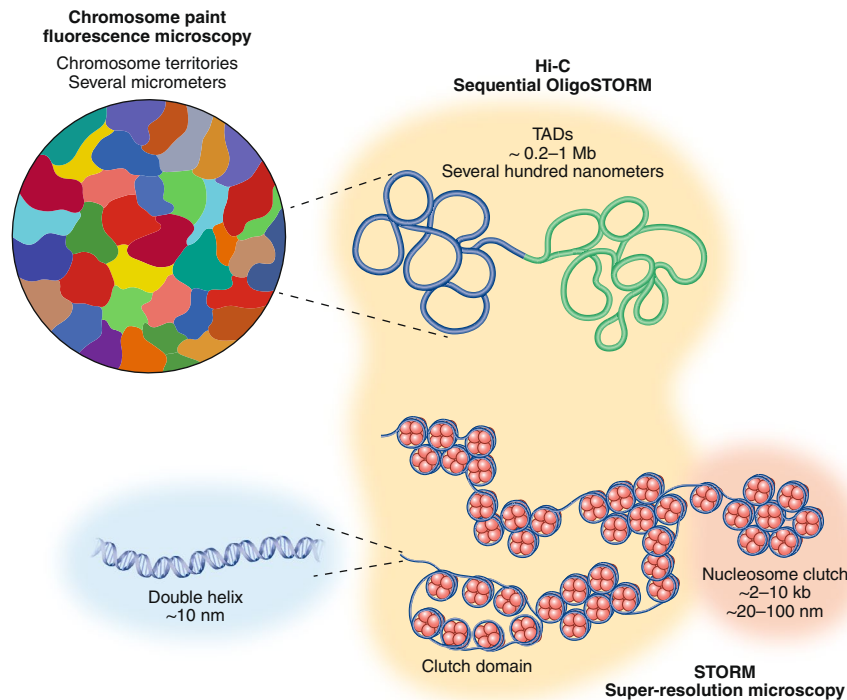


**Fig. 1 | Artist's rendering of the different levels of genome organization and the methodologies that have identified each organizational unit.** As revealed by chromosome painting and fluorescence microscopy, individual chromosomes occupy specific regions, known as chromosome territories, that are several micrometers in length. Genomic approaches and super-resolution imaging revealed the existence of topologically associating domains (TADs) in the size range of tens of kilobases to megabases, or several hundred nanometers. Super-resolution imaging further revealed nanodomains of nucleosomes (nucleosome clutches) of around a few kilobases in genomic size, as well as the clustering of these nanodomains in close proximity to form larger domains with a size range similar to that of TADs.

with distant cis-regulatory elements (that is, enhancers), and these promoter–enhancer contacts are thought to be important in regulating gene activity<sup>16</sup>. Several ‘architectural’ proteins have been identified that are responsible for organizing and defining the boundaries of these domains. In particular, Hi-C revealed that TADs and loops are dependent on the cohesin complex and on CTCF<sup>17–20</sup>. Cohesin is a multisubunit protein complex that forms a ring-shaped structure, while CTCF (CCCTC-binding factor) is a highly conserved DNA-binding protein. Depletion of cohesin subunits or CTCF leads to loss of all TADs and loops<sup>19–23</sup>. The prevailing model is that cohesin rings embrace DNA, loops are extruded through the rings and loop extrusion stops when cohesin encounters two CTCF proteins bound on either end of the DNA in a convergent orientation<sup>24,25</sup>. Although the exact details of this model are debated, *in vitro* experiments have shown that the cohesin loader NIBPL and cohesin together can extrude DNA loops in the presence of ATP<sup>26,27</sup>.

Although 3C methods have dramatically improved our understanding of 3D genome organization, they provide only an average view over millions of cells, obscuring details of single-cell heterogeneity and analysis of rare cell populations. In addition, these methods do not preserve the relation of genomic regions to important nuclear landmarks, including the nuclear lamina and the nucleoli. Finally, the nucleosome-level structure of organizational units uncovered by Hi-C remains unresolved, although this limitation may be overcome by a recently developed method called micro-C, which uses micrococcal nuclease rather than restriction enzymes to cut DNA at hypersensitive sites in between nucleosomes<sup>28</sup>. The remaining limitations and questions are starting to be further addressed with the recent revolutions in light microscopy and labeling

technologies that are now allowing us to visualize the smallest organizational units of chromosomes *in vivo*.

#### Electron microscopic view of genome organization

Given the high density of nucleic acids and proteins inside the nucleus, it has been difficult to use electron microscopy to visualize chromosome structure in intact cells because of low contrast. As a result, many early electron microscopy studies of higher-order chromatin folding were carried out on chromatin fibers reconstituted *in vitro*, in which nucleosomes were assembled together with plasmids containing strong nucleosome positioning sequences and further compacted through the addition of linker histones under specific ionic strength conditions<sup>29</sup>. Alternatively, electron micrographs of nuclei isolated from hypotonically lysed cells and treated with MgCl<sub>2</sub> were used<sup>30</sup>. These studies converged on the model that chromatin folds into a 30-nm fiber. However, cryo-electron microscopic imaging of chromosomes *in situ* revealed a homogenous, grainy texture containing features at the size scale of 11 nm and no superstructure or periodic order<sup>31,32</sup>. Further, 3D electron tomography of *Xenopus laevis* egg extracts revealed 30–40-nm domains consisting of nucleosome clusters<sup>33</sup>. Finally, electron spectroscopic imaging of mouse somatic cells was consistent with the open and closed chromatin being made up of 10-nm rather than 30-nm fibers<sup>34</sup>. All these experiments put into doubt the hierarchical folding model of chromatin and the existence of a regular 30-nm fiber structure. The most recent evidence against the hierarchical folding and 30-nm fiber model came from super-resolution imaging of nucleosomes in intact nuclei (see more below)<sup>35</sup> and subsequently from electron tomographic imaging of DNA stained with an

electron-microscopy-compatible dye that resolved the contrast problem (ChromEMT)<sup>36</sup>.

### Imaging global genome organization at high resolution with light microscopy

Super-resolution microscopy extended the spatial resolution of a light microscope from the ~250 to the 10–30-nm length scale, breaking what had been a fundamental limit. The underlying principles behind various super-resolution microscopy methods have been reviewed elsewhere<sup>37,38</sup>. These technologies, including structured illumination microscopy (SIM), single-molecule localization microscopy (SMLM, including STORM, PALM and DNA-PAINT) and stimulated emission depletion (STED) microscopy, have been applied to visualize features of nuclear organization that are smaller than the diffraction limit. In combination with newly developed labeling technologies, these super-resolution methods are providing a second revolution in parallel to 3C methods in our understanding of the genome organization.

STORM has been used to visualize the global organization of nucleosomes inside the nucleus (Fig. 2)<sup>35</sup>. These images revealed structures at varying length scales ranging from tens to hundreds of nanometers (Fig. 2a–c)<sup>35</sup>. The striking aspect of these early images was the absence of a prominent 30-nm fiber-like structure. Instead, nucleosomes were shown to form heterogeneous groups, which were named nucleosome clutches (Figs. 1 and 2b)<sup>35</sup>. Based on their spatial size (~30–50 nm) and the number of nucleosomes they contain, clutches correspond to a genomic length scale of a few kilobases, which is at the current limit of the spatial resolution of STORM. Clutches were interspersed with nucleosome-poor regions, and multiple clutches clustered in close proximity, forming larger “clutch domains” in the size range of several hundred nanometers (a genomic scale of tens of kilobases to megabases; Figs. 1 and 2a–c)<sup>39</sup>. It would be interesting to determine in future whether these clutch domains correspond to TADs and loops identified using Hi-C (Fig. 1). Clutch size and density were found to inversely correlate with cell pluripotency, suggesting that despite its heterogeneity, clutch organization is cell type specific<sup>35</sup>. The heterogeneous organization of nucleosomes in the form of nucleosome clutches uncovered by STORM is in stark contrast to the textbook model of ordered, hierarchical folding of the chromatin fiber. In line with the super-resolution results for nucleosomes, STORM imaging of individual chromosomes in which DNA was labeled with 5-ethynyl-2'-deoxyuridine (EdU) showed small, clustered nanodomains organized into larger domains (Fig. 2d), suggesting that DNA organization mirrors nucleosome organization<sup>40</sup>. Live-cell super-resolution imaging of nucleosomes also showed globular domains in the size range of hundreds of nanometers, resembling the clustered organization of multiple clutches (that is, clutch domains)<sup>41</sup>.

Multicolor STORM imaging was further used to correlate specific epigenetic modifications to chromatin compaction. These images revealed that silencing histone marks (H3K27me3) formed larger nanodomains that localized to more compacted DNA regions than active marks (H3K9ac, H3K4me3)<sup>42</sup>. These results are in line with earlier work showing that inhibition of histone deacetylase (HDAC) to induce hyperacetylation gives rise to smaller and less dense nucleosome clutches<sup>35,39</sup>. To further analyze the impact of histone tail acetylation on chromatin organization, nucleosomes were imaged together with DNA. This work showed that the compaction level of DNA within nucleosome clutches was independent of clutch size and instead depended on the level of acetylation of the histone tails<sup>39</sup>. In hyperacetylated cells, histone clutches not only were smaller but also contained DNA compacted to a lesser extent than in similar-sized clutches in wild-type (non-hyperacetylated) cells<sup>39</sup>. Interestingly, the biggest change in DNA compaction in hyperacetylated cells was observed within the clutch domains<sup>39</sup>. In combination, these results suggest that transcriptional activity and DNA

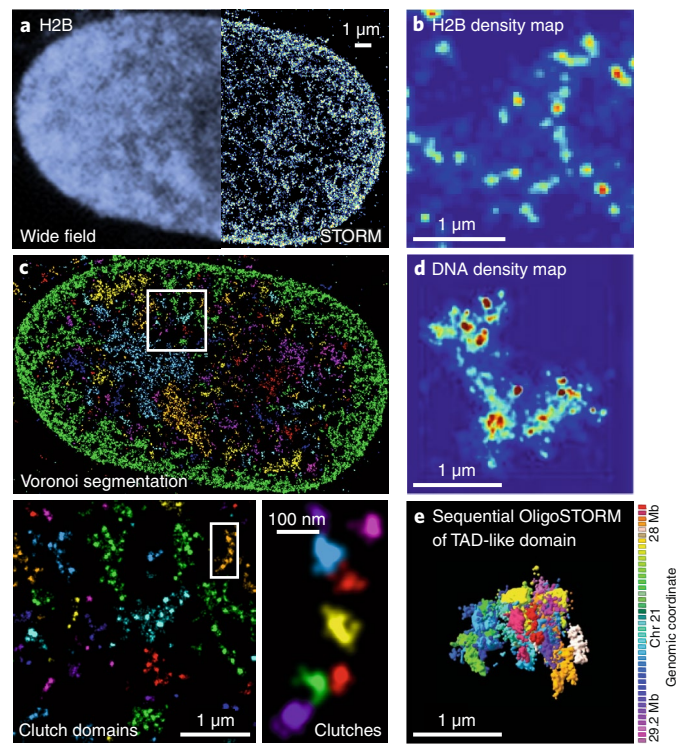


**Fig. 2 | Super-resolution imaging of histone and DNA organization.**

**a**, A comparison of wide-field and super-resolution image of the core histone protein H2B (unpublished images, Lakadamyali and Cosma laboratories). **b**, A density-based rendering of nucleosome organization shown in zoomed-in form (adapted with permission from ref. <sup>35</sup>, Elsevier). **c**, Segmentation of chromatin organization using Voronoi tessellation, in which localizations that share Voronoi polygons and hence are spatially connected are color coded with the same color. This segmentation reveals domains of varying size range. The largest domain is located at the nuclear periphery (green) and likely corresponds to constitutive heterochromatin. Smaller domains are visible in the nuclear interior (zoom-in of the white square) in the size range of TADs. Finally, these domains are composed of much smaller units (nanodomains) corresponding to small groups of nucleosomes (nucleosome clutches; zoom-in of the white rectangle). Unpublished images from Lakadamyali and Cosma laboratories. **d**, Super-resolution imaging of individual chromosomes labeled with EdU, showing nanodomains arranged in close proximity forming larger domains. Adapted with permission from ref. <sup>40</sup> (Ke Fang, Xuecheng Chen, Xiaowei Li, Yi Shen, Jielin Sun, Daniel M. Czajkowsky & Zhifeng Shao. Super-resolution imaging of individual human subchromosomal regions *in situ* reveals nanoscopic building blocks of higher-order structure. ACS Nano 12, 4909–4918). Copyright (2018) American Chemical Society. **e**, Sequential OligoSTORM image of a >1-Mb genomic region revealing globular TAD-like domains in single cells (adapted with permission from ref. <sup>48</sup>, AAAS).

accessibility are likely regulated at multiple levels: (i) at the level of clutch size, with the DNA within smaller clutches being more accessible; (ii) at the level of DNA compaction within the nucleosome clutches, with histone acetylation leading to less compaction and more accessibility of the underlying DNA; and (iii) at the level of clutch domains, which unfold and become more dispersed in hyperacetylated cells, leading to increased DNA accessibility.

### Imaging specific genomic regions at high resolution

Nucleosome and DNA labeling coupled with high-resolution imaging provides a global view of chromatin organization with near-nucleosome-level spatial resolution, but it does not provide sequence specificity, and hence it cannot be used to study

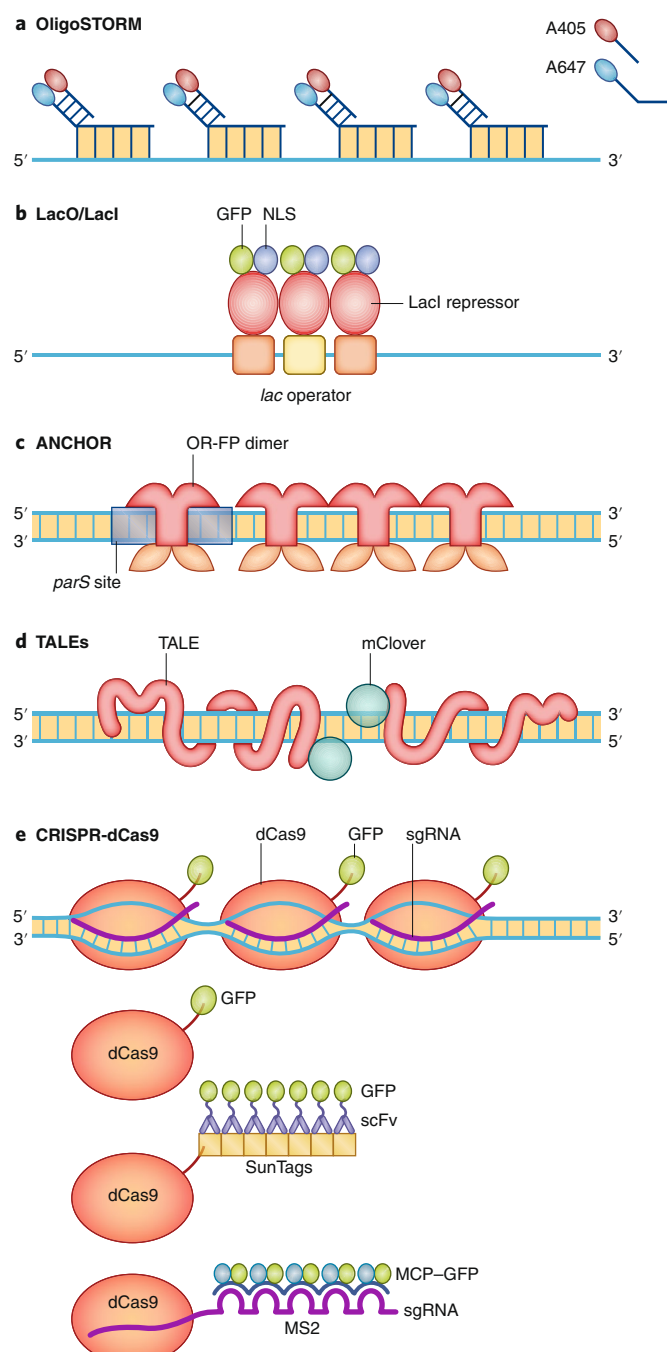
the organization of specific genomic regions. Fluorescence in situ hybridization (FISH) has long been used to visualize the spatial positioning of genomic loci and has revealed that genes tend to occupy specific regions within the nucleus, with silenced genes often closer to the nuclear lamina than active genes<sup>9,43</sup>. More recent high-throughput imaging has also revealed a good deal of heterogeneity in gene positioning<sup>44</sup>. Although FISH results correlate with Hi-C results—that is, regions with higher contact frequency in Hi-C tend to be closer in space on average—at a single-cell level these regions can be as far apart as regions with no enhanced contact frequency<sup>44</sup>. These results are compatible with the heterogeneity in genome folding that is observed at the genome-wide level by super-resolution microscopy and ChromEMT.

FISH as such has been limited to visualizing a subset of relatively small genomic regions ranging in size between 50 and 300 kb. This challenge was overcome with the advent of Oligopaints, small (32-mer) oligonucleotides with genomic homology (Fig. 3a)<sup>45,46</sup>. Combined Oligopaint and STORM imaging (OligoSTORM) revealed that genomic regions with different epigenetic states have distinct folding<sup>47</sup>. In this work, the genome was separated into active regions (enriched in H3K4me2 and H3K79me3 marks), repressed regions (enriched in H3K27me3 or Polycomb-group proteins) and inactive regions (lacking H3 modifications, transcription factors or Polycomb proteins). Oligopaint probes were designed for each state, and the volume occupied in space by each region was measured<sup>47</sup>. Repressed and inactive regions were more compacted and occupied a smaller volume than active regions. Thus, the folding of chromatin correlates with epigenetic state, although, interestingly, large regions of the genome depleted of specific histone H3 marks (denoted as inactive regions) also showed distinct patterns of folding and compaction from active and repressed regions, suggesting that factors other than epigenetic modifications also play roles in 3D genome folding.

Oligopaint can be used to ‘walk’ along chromosomes by sequentially hybridizing, imaging and extinguishing oligo probes<sup>48–51</sup>. This approach helps trace the folding of genomic DNA through 3D space. The step size of the walk can be tuned to walk either along

**Fig. 3 | Artist's rendering of the methods for visualizing specific genomic sites.** **a**, Oligopaints and OligoSTORM: Oligopaints are bioinformatically designed and synthesized small (32-mer) oligonucleotides with genomic homology. They can be designed with high specificity, high genomic coverage and high density, making it possible to label genomic regions ranging in size from a few tens of kilobases to megabases. This enables both conventional and super-resolution microscopy, including STORM when linked to photoswitchable fluorophore pairs such as Alexa Fluor 405-Alexa Fluor 647. **b**, lac operator (LacO)-lac repressor (LacI): LacO consists of a repetitive gene array, which can be incorporated into the genome and is specifically recognized and bound by LacI. Fusing LacI to a fluorescent protein such as green fluorescent protein (GFP) enables visualization of the genomic region containing LacO. **c**, ANCHOR system: The bacterial ParB proteins bind as dimers to palindromic 16-bp sequences (*parS*). ParB can be fused to a fluorescent protein (OR-FP), in which case the binding of OR-FP dimers acts as a seed, recruiting further ParB proteins that bind nonspecifically to adjacent DNA and hence enhance the signal at the locus. **d**, Transcription activator-like effector (TALE) domain: TALEs are sequence-specific DNA-binding proteins in which each 33–35-aa repeat binds to a specific base pair. Multiple TALEs can thus be assembled in a modular fashion to bind to a specific genomic sequence and further fused to a fluorescent protein to enable visualization. **e**, CRISPR-dCas9: An enzymatically deactivated version of Cas9 (dCas9) is fused to a fluorescent protein and recruited to the specific locus through the use of a guide RNA (gRNA) sequence. Signal can be enhanced via the use of SunTag or MS2 loops incorporated into the gRNA. scFv, single-chain variable fragment; MCP, methyl-accepting chemotaxis protein.

megabase domains with larger steps and hence lower spatial resolution<sup>51</sup> or, by using a finer step size, along smaller kilobase domains with much higher spatial resolution<sup>49</sup>. This approach was first used to label successive TADs within a chromosome to determine their spatial organization<sup>51</sup>. Later, megabase regions containing multiple TADs and sub-TADs were labeled in finer steps of 30 kb and imaged sequentially using OligoSTORM<sup>48</sup>. Remarkably, these images revealed globular TAD-like domains in single cells (Fig. 2e), consistent with super-resolution images of TADs in *Drosophila melanogaster*<sup>52</sup>. The centroid-to-centroid distance between each 30-kb segment was then measured, and finally a spatial interaction heat map was created from the distance scores<sup>48</sup>. These heat maps, when averaged over hundreds of cells, were highly compatible with Hi-C heat maps of the same region, revealing TADs with strong boundaries at CTCF and cohesin sites<sup>48</sup>. Surprisingly, however, heat



maps generated from individual cells showed highly heterogeneous boundaries, in which a boundary had a nonzero probability of being positioned at any genomic site but with a slight bias toward being positioned at cohesin or CTCF sites<sup>48</sup>. Strikingly, depletion of cohesin did not eliminate globular TAD-like structures in single cells but made their boundary positions more variable, with no preference for CTCF sites.

Walking along much larger regions with larger steps and imaging with STORM also showed that chromosome folding at these large length scales is highly variable even between two alleles of the same chromosome<sup>50</sup>. Although on average there is a correlation between the active A compartments and inactive B compartments assigned by Hi-C and the spatial entanglement or separation of these compartments in the imaging data, there is also a high degree of heterogeneity in the spatial organization of A and B compartments at the single-cell level<sup>50</sup>. Therefore, tracing the path of genomic regions with varying step sizes using sequential FISH indicated that at the ensemble average level, there is remarkable agreement between imaging and genomic methods, revealing domains and interactions within single cells. These chromosome walk approaches further illustrate the variability of domain boundaries at the level of single cells and clearly show that cohesin is not that critical for the maintenance or formation of these clustered domains.

Recently, the resolution of chromosome walks was pushed to the kilobase scale by walking with much smaller step sizes (2–10 kb) in an impressive method called optical reconstruction of chromatin architecture (ORCA)<sup>49</sup>. ORCA was used to reconstruct genomic regions in cryosections of *Drosophila* embryos and match genome architecture to cell-type-specific gene-expression profiles by combining the DNA imaging with highly multiplexed RNA FISH<sup>49</sup>. Perhaps most surprisingly, this approach revealed that although the physical proximity of a promoter to its enhancer was somewhat predictive of active transcription, the correlation was weak, and many active promoters were not in physical proximity to their enhancers<sup>49</sup>. These results suggest that promoter–enhancer interactions likely are highly dynamic rather than involving the formation of stable loops (see more below).

There are remaining challenges with this type of ‘domain painting’ approach, including efficient multiplexing of DNA and protein labeling. The denaturing conditions used in Oligopaint can be detrimental to some proteins, making it hard to label them with sufficient efficiency for subsequent high-resolution imaging. In addition, these methods currently require specialized equipment, limiting their wide accessibility. Finally, low efficiency of hybridization of the Oligopaint probes, which becomes more problematic as the probe size becomes smaller, can lead to many segments being missing from the imaged regions.

### Computational modeling of chromosome structure

Computational models play an important role in enriching our understanding of chromosome structure, especially in the current era in which researchers are trying to interpret rich experimental datasets obtained from 3C and imaging approaches. These models have been reviewed extensively elsewhere<sup>53–56</sup>, and hence we aim here merely to provide a broad overview of the general classes of models and discuss future challenges. Models can range in scale from all-atom molecular dynamics simulations of individual nucleosomes, to mesoscale coarse-grained models of oligonucleosome fibers consisting of tens or hundreds of nucleosomes, to even coarser polymer and continuum models of megabase-sized regions<sup>55</sup>. Coarse-grained models of oligonucleosome fibers may be compared to super-resolution images of nucleosome clutches, whereas polymer and continuum models may better capture domain features at the scale of TADs.

The models can be further categorized based on whether they incorporate experimental data as input parameters. Data-driven models use Hi-C maps, or in some cases imaging data, to put

constraints on pairwise distances between sequences so as to convert contact maps into distance maps and to finally generate a single consensus structure or an ensemble of most probable structures<sup>53</sup>. De novo models, on the other hand, use a set of physical principles to simulate an ensemble of structures, and the compatibility of these structures with Hi-C or imaging data is determined afterwards<sup>53</sup>. This class of models includes the fractal globule model and loop-extrusion models<sup>24,57</sup>. De novo models inform our mechanistic understanding of the folding principles of the genome, making valuable predictions that can potentially be experimentally tested. However, these models often recapitulate genome folding only at a specific length scale<sup>53</sup>. Data-driven models, meanwhile, have their own pitfalls. For example, they are often guided by Hi-C maps, which provide only an average spatial map from a large population of cells, and may have insufficient resolution in terms of abundance of contacts. Although some models have incorporated constraints from imaging data<sup>50</sup>, currently there are not enough high-throughput and high-resolution FISH-based imaging data to guide data-driven models. In the future, integrating data from both genomic and imaging studies may help enrich the input data and produce more precise models of chromosome structure.

### Live-cell imaging of genome dynamics

The main drawback of FISH-based approaches is that they can only be used in fixed cells and hence cannot reveal information about genome dynamics. Visualizing specific genomic regions in living cells requires a labeling system that does not rely on denaturing conditions coupled with the accumulation at the genomic site of sufficient fluorescent molecules over background to enable efficient detection. Artificial gene arrays have been a valuable tool that satisfies these criteria. In particular, the *lac* operator (LacO)/*lac* repressor (LacI) system from *Escherichia coli* has been widely used to visualize chromatin dynamics and DNA–protein interactions (Fig. 3b)<sup>58</sup>. However, though useful, this system has important drawbacks, specifically that the high number of repeats present in the LacO sequence can disrupt chromatin organization/function and, importantly, that this system is often inserted in the genome in multiple copies at random locations and is not suitable for visualizing endogenous genomic sites. Alternatively, the Anchor (ParB/*parS*) system takes advantage of protein oligomerization at a site-specific locus, rather than a repetitive gene array, to achieve the signal amplification needed to visualize that locus (Fig. 3c)<sup>59</sup>. Despite not involving a large repetitive gene array, the *parS* sequence still needs to be incorporated into the genome, and doing so at a specific locus without perturbing the locus dynamics, organization and function may be challenging.

More recently, methods have been developed that can label endogenous genomic loci without the need to incorporate non-native sequences into the genome. It is, however, important to mention that some of these methods (such as CRISPR) may still perturb the gene locus structure because they may lead to disruptions of the DNA duplex upon guide RNA (gRNA) hybridization. These methods rely on DNA-binding proteins such as transcription activator-like effector (TALE) domain proteins or the enzymatically deactivated version of CRISPR-associated protein 9 (dCas9; Fig. 3d,e)<sup>60,61</sup>. Both approaches have been used successfully to label genomic regions that contain highly repetitive sequences, such as centromeres or telomeres. The specificity of CRISPR-dCas9 to the genomic region is mediated solely by gRNAs, making this approach much simpler than the use of TALEs. Hence, recent effort has focused on optimizing and multiplexing CRIPR-dCas9 for genome visualization<sup>62–65</sup>. For example, the use of orthogonal dCas9 systems or the incorporation of RNA aptamers into the gRNA enable multi-color imaging of different genomic regions<sup>63,65</sup>.

A main challenge has been adapting this approach to label nonrepetitive regions of the genome. Initial work showed that to

accumulate detectable signal at the locus, ~30 gRNAs were required to tile along the genomic region<sup>60</sup>. Delivering these gRNAs into the cell requires transfections with multiple plasmids, markedly decreasing labeling efficiency. Several groups have undertaken the challenges both of boosting the number of gRNAs that can be delivered using a single plasmid and of using amplification methods to enhance the signal at the gene locus. Enhanced signal has been achieved by combining CRISPR-dCas9 with SunTag, as well as by incorporating repetitive aptamers into the gRNA (Fig. 3e)<sup>64–66</sup>. SunTag labeling, for example, has enabled super-resolution imaging of low-repeat regions and estimation of telomere length in different cell types<sup>64</sup>. CRISPR-Tag used CRISPR-targetable repeats from *Caenorhabditis elegans* incorporated into the gene locus as a universal, efficient tag to label genomic regions<sup>62</sup>. In parallel, chimeric array of gRNA oligonucleotides (CARGO) was developed to deliver 12 or more gRNAs in a highly multiplexed fashion using a single plasmid<sup>67</sup>. This approach has been used to label gene promoters and cis-regulatory elements (enhancers) with a sufficient signal-to-background ratio to visualize their dynamics in live cells<sup>67</sup>. These studies showed that the mobility of promoters and enhancers is linked to their transcriptional state, with higher transcriptional activity leading to greater mobility<sup>67</sup>. These results suggest that RNA polymerase II (RNA Pol II) may induce ‘stirring’ and increased genomic mobility<sup>67</sup>. Such a mechanism may ensure robust transcription by increasing the frequency with which enhancers bump into their promoters. However, recent super-resolution chromatin tracing<sup>49</sup> (described above) and live-cell imaging of Sox2 and its control region<sup>68</sup> revealed that transcriptional activation of the promoter can occur in the absence of physical proximity between the promoter and the enhancer. Further work is needed to reconcile the enhanced loop formation between active enhancers and promoters detected using Hi-C and the lack of correlation between enhancer–promoter proximity and transcriptional activation observed through super-resolution and live-cell imaging in single cells.

### Single-molecule tracking of chromatin–protein interactions

Although our ability to tag and visualize endogenous genomic loci in living cells is relatively new, live-cell imaging of chromatin-interacting proteins, including transcription factors, architectural proteins and polymerases, has made a huge impact on our understanding of protein dynamics inside the nucleus. The protein of interest is typically tagged with a Halo- or SNAP-tag, under-labeled using the Halo/SNAP substrate such that single proteins can be visualized sparsely and their motion inside the nucleus tracked<sup>69,70</sup>. The residence times of transcription factors on DNA typically showed biexponential kinetics with a short (hundreds of milliseconds) and a long-lived (tens of seconds) binding time, interpreted as reflecting nonspecific and specific DNA interactions<sup>70</sup>. Overall, these experiments posited that transcription factors likely find their target sites through a process dominated by 3D diffusion in which they spend most of their time diffusing through the nucleus and sampling many nonspecific sites before engaging with a specific target site<sup>70</sup>. These studies were extended to live-cell super-resolution imaging to visualize the dynamics and spatial organization of RNA Pol II in the nucleus<sup>71</sup>. RNA Pol II formed transient clusters whose lifetime correlated with the mRNA output<sup>72</sup>. Follow-up work showed that at least some RNA Pol II clusters were phase-separated liquid-droplet condensates<sup>73</sup>. Mediator, a transcriptional coactivator, was also shown to form phase-separated liquid droplets that colocalized with Pol II droplets at super-enhancers<sup>73,74</sup>. The enhancer thus may not need to physically contact the promoter but rather may be present inside a phase-separated transcriptional droplet to activate the promoter. These phase-separated droplets can be several hundreds of nanometers in size, and their presence may explain the lack of correlation between enhancer–promoter proximity and transcriptional activation. Tracking of architectural proteins such as cohesin

and CTCF further showed that these proteins, rather than forming stable complexes, are in fact highly dynamic<sup>75</sup>. These results suggest that the loops observed in Hi-C may be much more dynamic, forming and breaking apart often.

It would be very interesting in future to combine the CRISPR-dCas9-based gene labeling with single-molecule imaging of transcription factors, polymerases and coactivators, as well as imaging of the transcriptional output, to further dissect the hierarchies in promoter–enhancer positioning, transcription factor and transcriptional machinery binding, and transcriptional activation.

### Mechanisms that organize the genome

High-resolution and live-cell imaging studies have been uncovering several underlying determinants of genome organization. First, as described above, genome packing and nucleosome organization depend on epigenetic state, with repressed regions showing high levels of folding and compaction that increase with genomic length<sup>47</sup>. Acetylation marks correspond to small nucleosome clutches with lower DNA compaction<sup>35,39,42</sup>. It is likely that the epigenetic state of the histones alone likely influences nucleosome packing by modulating the electrostatic charges and influencing nucleosome–nucleosome and nucleosome–DNA interactions. In addition, these modified histones may be bound by additional repressive factors, such as the Polycomb group proteins, that can further modify chromatin folding and compaction.

Second, Hi-C showed that the compartmentalization of the genome into TADs and loops is dependent on the architectural proteins cohesin and CTCF, which demarcate TAD and loop boundaries. However, super-resolution imaging and chromatin tracing revealed a more complex picture of TAD architecture in single cells, with highly variable boundaries that persisted after cohesin depletion<sup>48</sup>. More recent studies also revealed a similar picture in which neighboring TADs intermingled extensively with each other<sup>76</sup>. Even more surprisingly, depletion of cohesin leads to a reduction in the intermingling between neighboring TADs, rather than inducing ectopic interactions, as would be expected from the global loss of TADs observed in Hi-C<sup>76</sup>. Overall, architectural proteins such as cohesin and CTCF do seem to play an important role in genome organization, but the precise principles of how these proteins cooperate to organize the genome are still being uncovered. In particular, recent imaging work is revealing a more complicated picture than Hi-C, in which the proteins do not seem to form stable loops and TADs with well-defined boundaries in single cells.

Third, at a larger scale, the genome is compartmentalized and spatially segregated into active euchromatin and inactive heterochromatin, but it is likely that this binary classification is over-simplistic, and there are different flavors of hetero- and euchromatin with different levels of compaction and spatial organization. Epigenetic marks likely play a role at this level of organization as well, because TADs with similar histone marks tend to organize within the same compartment<sup>14,51</sup>. Phase separation is also emerging as a major player in hetero- and euchromatin segregation. Beside the fact that transcriptional machinery forms phase-separated droplets, it has been shown that linker histone H1 and the heterochromatin protein HP1 can phase separate<sup>77</sup>, and this phase separation may play a role in the formation of heterochromatin, given that nucleosomes seem to preferentially partition into the HP1 droplets but transcription factors show no preference<sup>77</sup>. In addition, transcription itself may create domains of high nascent RNA density around the transcriptionally active regions and may help organize euchromatin around those domains through phase separation<sup>78</sup>. Hence, although the organization of the genome is an important determinant of transcription, transcription itself can also shape genome organization. Finally, nucleosome arrays themselves phase separate in vitro under physiological salt concentrations, and liquid droplet formation by these arrays is enhanced by linker histone H1 and disrupted by

histone acetylation<sup>79</sup>. The *in vivo* relevance of phase separation in the formation of nucleosome and chromatin domains observed at multiple length scales remains to be determined.

### Conclusions, open questions and future perspectives

We are at an exciting time in which the development of new methods, including light and electron microscopy as well as genomic approaches, are elucidating longstanding questions about how the folding of the genome relates to gene activity. Single-cell imaging is more targeted and lower in throughput than genomic approaches such as Hi-C, allowing visualization of only a few genomic regions at a time in a small population of cells. However, these methods are inherently well suited to studying heterogeneity in genome folding, as well as genome organization, in rare cell populations such as cells undergoing reprogramming to pluripotency. The information obtained from imaging and genomic approaches has often been consistent; however, there have also been cases in which the two approaches generated seemingly contradictory results<sup>80</sup>. This discrepancy may be due to the fact that the single-cell view from microscopy and the population-average view from genomics are difficult to compare considering cell-to-cell heterogeneity and the dynamics of genome folding. This challenge is particularly exacerbated by the fact that genomics methods capture sequences especially when they are in very close contact, whereas microscopy methods capture the spatial distance of these sequences with the same frequency whether they are in close contact or not. To unify the view from these two approaches, it is important to more clearly define what contact frequency in 3C corresponds to in terms of spatial distance in imaging. Typically, a distance threshold (~200 nm) is used to define contact in imaging data, but this may be too large for actual contact as measured by genomic approaches.

Further, it is essential to bridge the gap in the throughput of the imaging and genomics methods. Recent advances that combine barcoding and high-resolution imaging have enabled multiplexed visualization of RNA transcripts at the level of the entire transcriptome<sup>81</sup>. Similar barcoding approaches combined with multiplexed multicolor imaging<sup>82–84</sup> and the use of microfluidics for automated *in situ* sample handling may in the near future also enable the visualization of many genes simultaneously in a large population of cells, making these approaches more compatible with genome-wide analysis. State-of-the-art examples in which genomic regions were visualized in thousands of cells at high resolution<sup>44,47,50</sup> have already demonstrated how the heterogeneity of TADs in single cells can be reconciled with the well-defined TAD boundaries observed at the population level in Hi-C<sup>48</sup>. Similar approaches, in which the single cell view can be compared to the population average view in a high-content imaging dataset of thousands or millions of cells, will help further clarify how emergent properties of genome folding can arise from seemingly heterogeneous single-cell data. In addition, future advances in single-cell Hi-C<sup>85</sup> can potentially enable more direct comparison between imaging and genomic approaches. Finally, the integration of genomic and imaging data through data-driven modeling and the development of *de novo* models compatible with both types of datasets can further guide our understanding of the mechanisms that shape genome organization.

Another interesting future challenge would be to determine whether the heterogeneity in genome folding observed in single cells has a functional consequence for transcriptional activation. Elucidating the exact mechanisms involved in shaping genome organization and the interplay between the various proposed mechanisms (architectural proteins, epigenetic modifications, phase separation) is another important challenge.

Despite its heterogeneity, chromatin organization at the nanoscale level is highly cell type specific and correlates with cell pluripotency<sup>35</sup>. It would be interesting to determine how the folding of the genome is actively and dynamically remodeled during

differentiation and cellular reprogramming, what the molecular players involved in the remodeling are and whether this remodeling is indeed the determinant of gene-expression profiles and cell fate. Such studies may enable the direct manipulation of cell fate through manipulation of genome folding, potentially leading to enhanced reprogramming. For example, during *in vivo* reprogramming in the oocyte-to-zygote transition in mice, it was shown that chromatin conformation is reorganized and is distinct in paternal and maternal pronuclei. TADs and loops, but not compartments, were shown to be present in zygotic maternal chromatin<sup>86</sup>. Another exciting prospect is to study how disruptions in the spatial organization of the genome may be pathological and lead to diseases including cancer or neurological disorders. Indeed, Hi-C showed that short-term repeats that become expanded in diseases such as fragile X syndrome are found at domain boundaries of TADs, and these boundaries are severely disrupted in disease states, implying a correlation between chromatin architecture and repeat-expansion diseases<sup>87</sup>. Oligopaint imaging showed that reduced intermixing of TADs upon cohesin loss affects the transcriptional bursting of genes near domain boundaries, which can potentially explain gene-expression changes observed in the cohesinopathy Cornelia de Lange syndrome<sup>76</sup>.

Although we have advanced in our ability to visualize DNA, RNA and proteins such as transcription factors in cells, we still do not have an easy-to-use, plug-and-play-type unified platform that enables simultaneous visualization of all these components at high resolution in living cells. Such a tool could potentially revolutionize our understanding of the hierarchies involved in activating and repressing transcription. In addition, the spatial resolution of most super-resolution microscopy methods is still not at the molecular scale and hence is not sufficient to resolve individual nucleosomes. New advances that provide ultra-high resolution, such as 3D MINFLUX<sup>88</sup>, may potentially be revolutionary for studying the smallest scales of genome folding. Similarly, tools making it possible to manipulate and rewire the genome at will are at their infancy<sup>51,89</sup>. New methods that can disrupt or form specific loops upon stimulation<sup>89</sup>, change the nucleosome-level compaction of chromatin fiber at specific loci, or dissolve or reform new chromatin domains will open a new window into genome structure, allowing us to go beyond correlations and study the cause-and-effect relationship between genome organization and transcriptional activation.

Overall, we are in an exciting time in which the development of new tools is driving huge progress in our understanding of genome architecture. It will be fascinating to see how existing and new cutting-edge biochemical and imaging tools will advance our understanding of the link between genome architecture and gene activity in physiology and disease states.

Received: 5 August 2019; Accepted: 22 January 2020;  
Published online: 2 March 2020

### References

- Olins, A. L. & Olins, D. E. Spheroid chromatin units (v bodies). *Science* **183**, 330–332 (1974).
- Woodcock, C. L. & Ghosh, R. P. Chromatin higher-order structure and dynamics. *Cold Spring Harb. Perspect. Biol.* **2**, a000596 (2010).
- Bannister, A. J. & Kouzarides, T. Regulation of chromatin by histone modifications. *Cell Res.* **21**, 381–395 (2011).
- Filion, G. J. et al. Systematic protein location mapping reveals five principal chromatin types in *Drosophila* cells. *Cell* **143**, 212–224 (2010).
- Kundaje, A. et al. Integrative analysis of 111 reference human epigenomes. *Nature* **518**, 317–330 (2015).
- Breiling, A., Turner, B. M., Bianchi, M. E. & Orlando, V. General transcription factors bind promoters repressed by Polycomb group proteins. *Nature* **412**, 651–655 (2001).
- Cremer, T. & Cremer, M. Chromosome territories. *Cold Spring Harb. Perspect. Biol.* **2**, a003889 (2010).
- Padeken, J. & Heun, P. Nucleolus and nuclear periphery: Velcro for heterochromatin. *Curr. Opin. Cell Biol.* **28**, 54–60 (2014).

9. Boyle, S. et al. The spatial organization of human chromosomes within the nuclei of normal and emerin-mutant cells. *Hum. Mol. Genet.* **10**, 211–219 (2001).
10. Chambeyron, S. & Bickmore, W. A. Chromatin decondensation and nuclear reorganization of the HoxB locus upon induction of transcription. *Genes Dev.* **18**, 1119–1130 (2004).
11. Grob, S. & Cavalli, G. Technical Review: A hitchhiker's guide to chromosome conformation capture. *Methods Mol. Biol.* **1675**, 233–246 (2018).
12. Furey, T. S. ChIP-seq and beyond: new and improved methodologies to detect and characterize protein-DNA interactions. *Nat. Rev. Genet.* **13**, 840–852 (2012).
13. Rao, S. S. et al. A 3D map of the human genome at kilobase resolution reveals principles of chromatin looping. *Cell* **159**, 1665–1680 (2014).
14. Lieberman-Aiden, E. et al. Comprehensive mapping of long-range interactions reveals folding principles of the human genome. *Science* **326**, 289–293 (2009).
15. Kalhor, R., Tjong, H., Jayathilaka, N., Alber, F. & Chen, L. Genome architectures revealed by tethered chromosome conformation capture and population-based modeling. *Nat. Biotechnol.* **30**, 90–98 (2011).
16. Rowley, M. J. & Corces, V. G. Organizational principles of 3D genome architecture. *Nat. Rev. Genet.* **19**, 789–800 (2018).
17. de Wit, E. et al. CTCF binding polarity determines chromatin looping. *Mol. Cell* **60**, 676–684 (2015).
18. Guo, Y. et al. CRISPR Inversion of CTCF sites alters genome topology and enhancer/promoter function. *Cell* **162**, 900–910 (2015).
19. Rao, S. S. P. et al. Cohesin loss eliminates all loop domains. *Cell* **171**, 305–320.e324 (2017).
20. Schwarzer, W. et al. Two independent modes of chromatin organization revealed by cohesin removal. *Nature* **551**, 51–56 (2017).
21. Gassler, J. et al. A mechanism of cohesin-dependent loop extrusion organizes zygotic genome architecture. *EMBO J.* **36**, 3600–3618 (2017).
22. Nora, E. P. et al. Targeted degradation of CTCF decouples local insulation of chromosome domains from genomic compartmentalization. *Cell* **169**, 930–944.e922 (2017).
23. Wutz, G. et al. Topologically associating domains and chromatin loops depend on cohesin and are regulated by CTCF, WAPL, and PDS5 proteins. *EMBO J.* **36**, 3573–3599 (2017).
24. Sanborn, A. L. et al. Chromatin extrusion explains key features of loop and domain formation in wild-type and engineered genomes. *Proc. Natl Acad. Sci. USA* **112**, E6456–E6465 (2015).
25. Fudenberg, G. et al. Formation of chromosomal domains by loop extrusion. *Cell Rep.* **15**, 2038–2049 (2016).
26. Davidson, I. F. et al. DNA loop extrusion by human cohesin. *Science* **366**, 1338–1345 (2019).
27. Kim, Y., Shi, Z., Zhang, H., Finkelstein, I. J. & Yu, H. Human cohesin compacts DNA by loop extrusion. *Science* **366**, 1345–1349 (2019).
28. Hsieh, T. H. et al. Mapping nucleosome resolution chromosome folding in yeast by Micro-C. *Cell* **162**, 108–119 (2015).
29. Song, F. et al. Cryo-EM study of the chromatin fiber reveals a double helix twisted by tetranucleosomal units. *Science* **344**, 376–380 (2014).
30. Scheffer, M. P., Eltsov, M. & Frangakis, A. S. Evidence for short-range helical order in the 30-nm chromatin fibers of erythrocyte nuclei. *Proc. Natl Acad. Sci. USA* **108**, 16992–16997 (2011).
31. McDowell, A. W., Smith, J. M. & Dubochet, J. Cryo-electron microscopy of vitrified chromosomes in situ. *EMBO J.* **5**, 1395–1402 (1986).
32. Maeshima, K. & Eltsov, M. Packaging the genome: the structure of mitotic chromosomes. *J. Biochem.* **143**, 145–153 (2008).
33. König, P., Braunfeld, M. B., Sedat, J. W. & Agard, D. A. The three-dimensional structure of in vitro reconstituted *Xenopus laevis* chromosomes by EM tomography. *Chromosoma* **116**, 349–372 (2007).
34. Fussner, E. et al. Open and closed domains in the mouse genome are configured as 10-nm chromatin fibres. *EMBO Rep.* **13**, 992–996 (2012).
35. Ricci, M. A., Manzo, C., García-Parajo, M. F., Lakadamyali, M. & Cosma, M. P. Chromatin fibers are formed by heterogeneous groups of nucleosomes in vivo. *Cell* **160**, 1145–1158 (2015).
36. Ou, H. D. et al. ChromEMT: visualizing 3D chromatin structure and compaction in interphase and mitotic cells. *Science* **357**, eaag0025 (2017).
37. Lakadamyali, M. & Cosma, M. P. Advanced microscopy methods for visualizing chromatin structure. *FEBS Lett.* **589**(20 Pt A), 3023–3030 (2015).
38. Oddone, A., Vilanova, I. V., Tam, J. & Lakadamyali, M. Super-resolution imaging with stochastic single-molecule localization: concepts, technical developments, and biological applications. *Microsc. Res. Tech.* **77**, 502–509 (2014).
39. Otterstrom, J. et al. Super-resolution microscopy reveals how histone tail acetylation affects DNA compaction within nucleosomes in vivo. *Nucleic Acids Res.* **47**, 8470–8484 (2019).
40. Fang, K. et al. Super-resolution imaging of individual human subchromosomal regions in situ reveals nanoscopic building blocks of higher-order structure. *ACS Nano* **12**, 4909–4918 (2018).
41. Nozaki, T. et al. Dynamic organization of chromatin domains revealed by super-resolution live-cell imaging. *Mol. Cell* **67**, 282–293.e287 (2017).
42. Xu, J. et al. Super-resolution imaging of higher-order chromatin structures at different epigenomic states in single mammalian cells. *Cell Rep.* **24**, 873–882 (2018).
43. Ferrai, C., de Castro, I. J., Lavitas, L., Chotalia, M. & Pombo, A. Gene positioning. *Cold Spring Harb. Perspect. Biol.* **2**, a000588 (2010).
44. Finn, E. H. et al. Extensive heterogeneity and intrinsic variation in spatial genome organization. *Cell* **176**, 1502–1515.e1510 (2019).
45. Beliveau, B. J. et al. Versatile design and synthesis platform for visualizing genomes with Oligopaint FISH probes. *Proc. Natl Acad. Sci. USA* **109**, 21301–21306 (2012).
46. Beliveau, B. J. et al. In situ super-resolution imaging of genomic DNA with OligoSTORM and OligoDNA-PAINT. *Methods Mol. Biol.* **1663**, 231–252 (2017).
47. Boettiger, A. N. et al. Super-resolution imaging reveals distinct chromatin folding for different epigenetic states. *Nature* **529**, 418–422 (2016).
48. Bintu, B. et al. Super-resolution chromatin tracing reveals domains and cooperative interactions in single cells. *Science* **362**, eaau1783 (2018).
49. Mateo, L. J. et al. Visualizing DNA folding and RNA in embryos at single-cell resolution. *Nature* **568**, 49–54 (2019).
50. Nir, G. et al. Walking along chromosomes with super-resolution imaging, contact maps, and integrative modeling. *PLoS Genet.* **14**, e1007872 (2018).
51. Wang, S. et al. Spatial organization of chromatin domains and compartments in single chromosomes. *Science* **353**, 598–602 (2016).
52. Szabo, Q. et al. TADs are 3D structural units of higher-order chromosome organization in *Drosophila*. *Sci. Adv.* **4**, eaar8082 (2018).
53. Imakaev, M. V., Fudenberg, G. & Mirny, L. A. Modeling chromosomes: beyond pretty pictures. *FEBS Lett.* **589**(20 Pt A), 3031–3036 (2015).
54. Marti-Renom, M. A. & Mirny, L. A. Bridging the resolution gap in structural modeling of 3D genome organization. *PLOS Comput. Biol.* **7**, e1002125 (2011).
55. Ozer, G., Luque, A. & Schlick, T. The chromatin fiber: multiscale problems and approaches. *Curr. Opin. Struct. Biol.* **31**, 124–139 (2015).
56. Nicodemi, M. & Pombo, A. Models of chromosome structure. *Curr. Opin. Cell Biol.* **28**, 90–95 (2014).
57. Mirny, L. A. The fractal globule as a model of chromatin architecture in the cell. *Chromosome Res.* **19**, 37–51 (2011).
58. Tsukamoto, T. et al. Visualization of gene activity in living cells. *Nat. Cell Biol.* **2**, 871–878 (2000).
59. Germier, T., Audibert, S., Kocanova, S., Lane, D. & Bystricky, K. Real-time imaging of specific genomic loci in eukaryotic cells using the ANCHOR DNA labelling system. *Methods* **142**, 16–23 (2018).
60. Chen, B. et al. Dynamic imaging of genomic loci in living human cells by an optimized CRISPR/Cas system. *Cell* **155**, 1479–1491 (2013).
61. Miyanari, Y., Ziegler-Birling, C. & Torres-Padilla, M. E. Live visualization of chromatin dynamics with fluorescent TALEs. *Nat. Struct. Mol. Biol.* **20**, 1321–1324 (2013).
62. Chen, B., Zou, W., Xu, H., Liang, Y. & Huang, B. Efficient labeling and imaging of protein-coding genes in living cells using CRISPR-Tag. *Nat. Commun.* **9**, 5065 (2018).
63. Ma, H. et al. Multicolor CRISPR labeling of chromosomal loci in human cells. *Proc. Natl Acad. Sci. USA* **112**, 3002–3007 (2015).
64. Neguembor, M. V. et al. (Po)STAC (Polycistronic SunTAg modified CRISPR) enables live-cell and fixed-cell super-resolution imaging of multiple genes. *Nucleic Acids Res.* **46**, e30 (2018).
65. Qin, P. et al. Live cell imaging of low- and non-repetitive chromosome loci using CRISPR-Cas9. *Nat. Commun.* **8**, 14725 (2017).
66. Tanenbaum, M. E., Gilbert, L. A., Qi, L. S., Weissman, J. S. & Vale, R. D. A protein-tagging system for signal amplification in gene expression and fluorescence imaging. *Cell* **159**, 635–646 (2014).
67. Gu, B. et al. Transcription-coupled changes in nuclear mobility of mammalian cis-regulatory elements. *Science* **359**, 1050–1055 (2018).
68. Alexander, J. M. et al. Live-cell imaging reveals enhancer-dependent *Sox2* transcription in the absence of enhancer proximity. *Elife* **8**, e41769 (2019).
69. Mazza, D., Ganguly, S. & McNally, J. G. Monitoring dynamic binding of chromatin proteins in vivo by single-molecule tracking. *Methods Mol. Biol.* **1042**, 117–137 (2013).
70. Liu, Z. & Tjian, R. Visualizing transcription factor dynamics in living cells. *J. Cell Biol.* **217**, 1181–1191 (2018).
71. Cisse, I. I. et al. Real-time dynamics of RNA polymerase II clustering in live human cells. *Science* **341**, 664–667 (2013).
72. Cho, W. K. et al. RNA Polymerase II cluster dynamics predict mRNA output in living cells. *Elife* **5**, e13617 (2016).
73. Cho, W. K. et al. Mediator and RNA polymerase II clusters associate in transcription-dependent condensates. *Science* **361**, 412–415 (2018).
74. Sabari, B. R. et al. Coactivator condensation at super-enhancers links phase separation and gene control. *Science* **361**, eaar3958 (2018).
75. Hansen, A. S., Pustova, I., Cattoglio, C., Tjian, R. & Darzacq, X. CTCF and cohesin regulate chromatin loop stability with distinct dynamics. *Elife* **6**, e25776 (2017).

76. Luppino, J.M. et al. Cohesin promotes stochastic domain intermingling to ensure proper regulation of boundary-proximal genes. Preprint at <https://doi.org/10.1101/649335> (2019).
77. Larson, A. G. et al. Liquid droplet formation by HP1 $\alpha$  suggests a role for phase separation in heterochromatin. *Nature* **547**, 236–240 (2017).
78. Hilbert, L. et al. Transcription organizes euchromatin similar to an active microemulsion. Preprint at <https://doi.org/10.1101/234112> (2018).
79. Gibson, B. et al. Organization of chromatin by intrinsic and regulated phase separation. *Cell* **179**, 470–484.e421 (2019).
80. Williamson, I. et al. Spatial genome organization: contrasting views from chromosome conformation capture and fluorescence *in situ* hybridization. *Genes Dev.* **28**, 2778–2791 (2014).
81. Chen, K. H., Boettiger, A. N., Moffitt, J. R., Wang, S. & Zhuang, X. RNA imaging. Spatially resolved, highly multiplexed RNA profiling in single cells. *Science* **348**, aaa6090 (2015).
82. Gómez-García, P. A., Garbacik, E. T., Otterstrom, J. J., García-Parajo, M. F. & Lakadamyali, M. Excitation-multiplexed multicolor superresolution imaging with fm-STORM and fm-DNA-PAINT. *Proc. Natl Acad. Sci. USA* **115**, 12991–12996 (2018).
83. Wade, O. K. et al. 124-color super-resolution imaging by engineering DNA-PAINT blinking kinetics. *Nano Lett.* **19**, 2641–2646 (2019).
84. Beghin, A. et al. Localization-based super-resolution imaging meets high-content screening. *Nat. Methods* **14**, 1184–1190 (2017).
85. Nagano, T. et al. Single-cell Hi-C reveals cell-to-cell variability in chromosome structure. *Nature* **502**, 59–64 (2013).
86. Flyamer, I. M. et al. Single-nucleus Hi-C reveals unique chromatin reorganization at oocyte-to-zygote transition. *Nature* **544**, 110–114 (2017).
87. Sun, J. H. et al. Disease-associated short tandem repeats co-localize with chromatin domain boundaries. *Cell* **175**, 224–238.e215 (2018).
88. Gwosch, K.C. et al. MINFLUX nanoscopy delivers 3D multicolor nanometer resolution in cells. *Nat. Methods* (2020).
89. Kim, J. H. et al. LADL: light-activated dynamic looping for endogenous gene expression control. *Nat. Methods* **16**, 633–639 (2019).

## Acknowledgements

This work was supported by the University of Pennsylvania Epigenetics Pilot Award (to M.L.), the Center for Engineering and Mechanobiology (CEMB), an NSF Science and Technology Center Pilot Award under grant agreement CMMI 15-48571 (to M.L.), a Linda Pechenik Montague Investigator Award (to M.L.), the European Union's Horizon 2020 Research and Innovation Programme (CellViewer No 686637 to M.L. and M.P.C.), Ministerio de Ciencia e Innovación, grant BFU2017-86760-P (AEI/FEDER, UE), and an AGAUR grant from Secretaria d'Universitats i Recerca del Departament d'Empresa i Coneixement de la Generalitat de Catalunya (2017 SGR 689 to M.P.C.). We acknowledge the support of the Spanish Ministry of Science and Innovation to the EMBL partnership, the Centro de Excelencia Severo Ochoa and the CERCA Programme / Generalitat de Catalunya.

## Competing interests

The authors declare no competing interests.

## Additional information

**Correspondence** should be addressed to M.L.

**Reprints and permissions information** is available at [www.nature.com/reprints](http://www.nature.com/reprints).

**Publisher's note** Springer Nature remains neutral with regard to jurisdictional claims in published maps and institutional affiliations.

© Springer Nature America, Inc. 2020